

## Comparing a Local Potential with a Non-Local Potential for the Bound States of $^{16}\text{O}$ and $^{40}\text{Ca}$

H. G. Cho,<sup>1</sup> B. Y. Moon,<sup>1</sup> K. S. Kim,<sup>2</sup> Myung-Ki Cheoun,<sup>3</sup> T. H. Kim,<sup>4</sup> and W. Y. So<sup>4,\*</sup>

<sup>1</sup>*Department of Optometry, Kangwon National University at Dogye, Samcheok 245-905, Korea*

<sup>2</sup>*School of Liberal Art and Science, Korea Aerospace University, Koyang 412-791, Korea*

<sup>3</sup>*Department of Physics, Soongsil University, Seoul 156-743, Korea*

<sup>4</sup>*Department of Radiological Science, Kangwon National University at Dogye, Samcheok 245-905, Korea*

(Received July 16, 2013; Revised October 7, 2013)

Using the non-local nuclear potentials, we calculate the binding energies and radial wave functions of a single particle, and the proton charge density for  $^{16}\text{O}$  and  $^{40}\text{Ca}$  nuclei. In order to obtain them, we use a matrix equation method generated from the integral form of the Schrödinger equation and find the best parameter set, which includes the potential depth, diffuseness, radius, and non-local parameter, by fitting the experimental data. The proton charge densities for the non-local potential are repulsive in comparison with those for the local potential. It is also found that the radius of the non-local potential is greater than that of the local one due to the non-local parameter ( $\beta$ ). In addition, using the trivially equivalent local potential (TELP) method, we compare the local potentials with the non-local potentials and then find that the non-local potentials are repulsive.

DOI: 10.6122/CJP.52.729

PACS numbers: 21.60.cs, 21.10-k, 25.30.Fj

To solve both bound and scattering problems including the exchange interaction between the projectile and the target [1, 2], one has to consider the non-locality. In general, the non-locality in most nuclear physics calculations is assumed to be small, except for the polarization potential [3–5]. For realistic nucleon-nucleon interactions, however, it is well known that the non-locality plays an important role in the calculation of nuclear properties [6, 7].

In Ref. [8], Perey and Buck introduced an approach such that the non-local potential was assumed to have a separable form and solved the wave equation numerically in its full integro-differential form, which is using an energy independent non-local optical potential. Using the Taylor expansion of the non-local potential and the non-local wave function in the non-local parameter ( $\beta$ ), they obtained the localized potential corresponding to the non-local potential. Franey and Ellis [9] suggested another localized potential method, the so-called trivially equivalent local potential (TELP) method. In this method, the localized wave function and the non-local wave function were assumed to be equal. Negele [10] introduced a position-dependent effective mass in the Schrödinger equation to replace the non-locality arising from the exchange term in the Hartree-Fock theory. He investigated the root-mean-square (rms) radii of the neutron wave functions at single-particle energies and the absolute magnitudes of the extreme tails of a Hartree-Fock theory, which includes

---

\*Electronic address: [wyso@kangwon.ac.kr](mailto:wyso@kangwon.ac.kr)

the exchange term. For nucleon and nuclei scattering, the local density, the local energy, or the local Slater exchange approximation is also used [6, 11]. Shlomo and Bertsch [12] calculated single particle binding energies of local and non-local potentials by using the random phase approximation (RPA) particle-hole theory of excitations. They applied this theory to the low multipolarities in  $^{16}\text{O}$ ,  $^{40}\text{Ca}$ , and  $^{208}\text{Pb}$ . As a result, they found that the width of the giant dipole in light nuclei is accounted for by the continuum, and the dipole decay width in heavy nuclei is small. So and Kim [7] calculated the binding energies and wave functions of the nuclear single particle, which were calculated for non-local nuclear potentials utilizing a matrix equation method for solving the integral equation derived from the Schrödinger equation in momentum space. As a result, they found that the non-local effect is radially repulsive for the nuclear density.

In our recent work [13], we calculated single particle binding energies and wave functions for  $^{208}\text{Pb}$  and compared our results with the experimental data obtained from Ref. [14] using the same technique as with the present method. An advantage of this work is that single particle binding energies can be found by using a simple Woods-Saxon potential considered Hartree-Fock effect instead of the complicated RPA theory using the particle-hole of excitations, as explained in Ref. [12].

As shown in Ref. [13], we calculated the single particle binding energies and proton charge densities for all the bound states of  $^{16}\text{O}$  and  $^{40}\text{Ca}$  by using a matrix equation method and the local potential for the bound states. In addition, we introduce the localized potential generated by using the TELP method. And then we compare the binding energies and the proton charge densities of the local with those of the non-local Schrödinger equation. Furthermore, we compare the local potential with the TELP which is replaced to the non-local potential.

In general, the non-local Schrödinger equation for bound states can be written as

$$-\frac{\hbar^2}{2\mu}\nabla^2\Psi(\vec{r}) + \int V(\vec{r}, \vec{r}')\Psi(\vec{r}')d\vec{r}' = E_n\Psi(\vec{r}), \quad (1)$$

where  $V(\vec{r}, \vec{r}')$  represents the non-local potential and  $E_n$  denotes the binding energy of the single particle. As shown in Refs. [7, 8, 13], we assume that the spin orbit and the Coulomb part in the non-local potential of Eq. (1) is used as the localized potential in this work. Thus, Eq. (1) is rewritten as

$$-\frac{\hbar^2}{2\mu}\nabla^2\Psi(\vec{r}) + \int V_0(\vec{r}, \vec{r}')\Psi(\vec{r}')d\vec{r}' + V_{\text{so}}(\vec{r})\Psi(\vec{r}) + V_c(\vec{r})\Psi(\vec{r}) = E_n\Psi(\vec{r}), \quad (2)$$

where the Coulomb potential  $V_c(\vec{r})$  is a usual form for a uniform charge distribution with the empirical rms radius, and  $V_{\text{so}}(\vec{r})$  is the spin-orbit potential. As shown by Perey and Buck [8], we used the non-local potential form as follows:

$$V_0(\vec{r}, \vec{r}') = W\left(\frac{|\vec{r} + \vec{r}'|}{2}\right)H(|\vec{r} - \vec{r}'|). \quad (3)$$

Here,  $W$  is a Woods-Saxon type function and  $H$  is a normalized Gaussian function given

by

$$H(|\vec{r} - \vec{r}'|) = \frac{1}{(\sqrt{\pi}\beta)^3} e^{-t^2}, \quad (4)$$

where  $\vec{t} = (\vec{r} - \vec{r}')/\beta$  and  $\beta$  is a non-local parameter. Note that the Gaussian function becomes a delta function when  $\beta$  approaches zero.

In order to solve the integro-differential equation of Eq. (2), we use the Fourier transform. In momentum space, Eq. (2) becomes as follows:

$$(k^2 + k_n^2)\Psi(\vec{k}) = -\frac{2\mu}{\hbar^2} \int V(\vec{k}, \vec{k}')\Psi(\vec{k}') d\vec{k}', \quad (5)$$

where  $\vec{p} = \hbar\vec{k}$  is the relative momentum and  $E_n = -\hbar^2 k_n^2/2\mu$  is the binding energy of the single particle in the nucleus. Wave functions are written as a function of the total angular momentum ( $j$ ), the orbital angular momentum ( $l$ ), and the spin ( $s$ ). After integrating the over all angle parts, we obtain a homogeneous Fredholm equation of the second type:

$$(k^2 + k_n^2)\psi_\alpha(k) = -\frac{2}{\pi} \int dk' k'^2 V_\alpha(k, k')\psi_\alpha(k'). \quad (6)$$

Here, the subscript  $\alpha$  includes the quantum numbers ( $n j l s$ ).

In order to solve this integral equation, we use the N-point Gaussian integration formula,

$$\int F(k)dk = \sum_j F(k_j)\omega_j, \quad (7)$$

where  $k_j$  are Gaussian integration points and  $\omega_j$  are weights. Then Eq. (7) can be written as a matrix equation [7],

$$\sum_{j=1}^N F_{ij} \phi_\alpha(k_j) = 0, \quad (8)$$

where

$$F_{ij} = \frac{2}{\pi} \frac{k_j^2}{k_i^2 + k_n^2} U_\alpha(k_i, k_j) \omega_j + \delta_{ij}. \quad (9)$$

Solving the eigen-value equation for Eq. (8), we can obtain binding energies and corresponding wave functions of the single particle in nuclei.

Next, the local Schrödinger equation for bound states can be written as

$$-\frac{\hbar^2}{2\mu} \nabla^2 \Psi(\vec{r}) + V_0(\vec{r})\Psi(\vec{r}) + V_{so}(\vec{r})\Psi(\vec{r}) + V_c(\vec{r})\Psi(\vec{r}) = E_n \Psi(\vec{r}). \quad (10)$$

TABLE I: Potential parameters for the local and the non-local potential.

System	Potential	Nucleon	$V_0$	$V_{so}$	$a_0 = a_{so}$	$r_0 = r_{so}$	$r_c$	$\beta$
$^{16}\text{O}$	Local	Proton	58.00	15.00	0.65	1.20	1.20	—
		Neutron	58.00	15.00	0.65	1.20	—	—
	Non-local	Proton	55.30	17.70	0.55	1.30	1.20	0.36
		Neutron	56.50	19.00	0.55	1.30	—	0.36
$^{40}\text{Ca}$	Local	Proton	57.00	15.00	0.65	1.20	1.20	—
		Neutron	57.00	15.00	0.65	1.20	—	—
	Non-local	Proton	58.90	18.85	0.75	1.25	1.20	0.36
		Neutron	57.80	16.35	0.75	1.25	—	0.36

We used the radial part of the local potential in Eq. (10), which is based on Shlomo and Bertsch's [12] work, as the Woods-Saxon type. It is given by

$$V(r) = \left[ \frac{V_0}{1 + \exp\left(\frac{r-R}{a}\right)} + \sigma \cdot \mathbf{L} \frac{1}{r} \frac{d}{dr} \left( \frac{V_{so}}{1 + \exp\left(\frac{r-R}{a}\right)} \right) \right] + \frac{1 - \tau_z}{2} V_c(r), \quad (11)$$

where  $\tau_z$  denotes the isospin of the nucleon, which is +1 and -1 for the neutron and the proton, respectively. Note that  $V_0$  and  $V_{so}$  are multiplied by a factor of  $(1 - 0.67 \frac{N-Z}{A} \tau_z)$  in comparison with the central potential and spin-orbit potential of Ref. [12]. Since  $^{16}\text{O}$  and  $^{40}\text{Ca}$  nuclei have the same number of protons and neutrons, the value of  $(1 - 0.67 \frac{N-Z}{A} \tau_z)$  becomes unity.  $a$  and  $r_0$  denote the diffuseness and the radius, respectively. These parameters are used in our calculation for the local potential. For the non-local potential, a detailed description on how to obtain the potential parameters will be described in the following paragraph.

In Ref. [13], we obtained three parameter sets with respect to the  $\beta$ -value, and it was found that the radius and the diffuseness increased with higher values of the non-local factor. In this work, we use the  $\beta$ -value with 0.36, because the non-locality effect cannot be shown when  $\beta$ -value approaches zero and the radius becomes quite large when the  $\beta$ -value is 0.85. Then we perform the  $\chi^2$  analysis using the six adjustable parameters, which are the depth, the diffuseness, and the radius of the central and spin-orbit potentials. After the first  $\chi^2$  fit, we can determine the radius as the average value of the radius for both potentials. Using the rest of the adjustable parameters except for the fixed radius parameter, we obtain the diffuseness parameter from the second  $\chi^2$  analysis. After the radius and the diffuseness parameters are determined, we can find the depth parameters using the last  $\chi^2$  analysis. The non-local potential of Table I shows parameters obtained in this fashion.

In Table I, the local and the non-local potential parameters are listed. Using these parameters, we reproduce the binding energies for the nuclear single particle in  $^{16}\text{O}$  and  $^{40}\text{Ca}$  nuclei of Ref. [12] at the first and second column from the right in Tables II and III.

TABLE II: Experimental and calculated proton binding energies (in MeV) for  $^{16}\text{O}$  and  $^{40}\text{Ca}$ .

nuclei	orbit	exp. [14]	Bertsch [12]		This work	
			local	non-local	local	non-local
$^{16}\text{O}$	$1s_{1/2}$	$40\pm 8$	31.86	27.62	29.36	30.27
	$1p_{3/2}$	18.4	16.79	18.45	14.71	16.44
	$1p_{1/2}$	12.1	11.72	12.12	9.89	11.17
$^{40}\text{Ca}$	$1s_{1/2}$	$50\pm 11$	35.37	35.48	33.75	34.78
	$1p_{3/2}$		24.85	23.32	23.41	24.51
	$1p_{1/2}$	$34\pm 6$	22.26	20.49	20.83	21.49
	$1d_{5/2}$		13.59	14.03	12.32	13.76
	$2s_{1/2}$	10.9	9.67	10.94	8.48	9.89
	$1d_{3/2}$	8.3	8.46	8.33	7.25	8.02

TABLE III: Experimental and calculated neutron binding energies (in MeV) for  $^{16}\text{O}$  and  $^{40}\text{Ca}$ .

nuclei	orbit	exp. [14]	Bertsch [12]		This work	
			local	non-local	local	non-local
$^{16}\text{O}$	$1s_{1/2}$		35.73	32.88	33.70	35.50
	$1p_{3/2}$	21.8	20.34	21.81	18.54	21.12
	$1p_{1/2}$	15.7	15.25	15.66	13.68	15.47
$^{40}\text{Ca}$	$1s_{1/2}$		43.63	43.51	42.71	42.68
	$1p_{3/2}$		32.68	32.07	31.76	31.72
	$1p_{1/2}$		30.14	29.31	29.25	29.15
	$1d_{5/2}$		20.98	21.32	20.09	20.27
	$2s_{1/2}$	18.1	17.04	18.14	16.24	16.76
	$1d_{3/2}$	15.6	15.89	15.69	15.06	15.32

In order to investigate the distinction between the local and non-local potential, we introduce the trivially equivalent local potential (TELP) method, which is a way to localize the non-local potential introduced by Franey and Ellis [9]:

$$V_0(r) = \frac{1}{\psi_\alpha^N(r)} \int dr' V_0(r, r') \psi_\alpha^N(r'), \quad (12)$$

under the assumption that the radial wave function of the local potential and that of the non-local potential are the same. Note that  $\psi_\alpha^N(r)$  is the radial wave function for the non-

local potential in Eq. (2), and the local and the non-local potential,  $V_0(r)$  and  $V_0(r, r')$ , are also  $\alpha$ -dependent. In order to use the local and the non-local radial wave functions, we can obtain the proton charge density [15, 16],

$$\rho_p^i(r) = \sum_{\alpha} \frac{n_p(\alpha)}{4\pi} |\psi_{\alpha}^i(r)|^2, \quad i = L \text{ or } N, \quad (13)$$

where  $n_p(\alpha)$  are the occupation proton numbers, and  $L$  ( $N$ ) means the local (non-local) potential. Note that the integration of the proton charge density becomes the proton number as follows:

$$\int_0^{\infty} \rho_p^i(r) d^3r = Z, \quad i = L \text{ or } N, \quad (14)$$

where  $Z$  is the proton number.

In order to calculate the binding energies and the wave functions for the non-local potential, we have to find the best parameter set for the non-local potential by fitting the experimental data. Then, we calculate the binding energies of the single particle in the  $^{16}\text{O}$  and  $^{40}\text{Ca}$  nuclei and compare with the experimental data in Table II and III. Our results for the local and the non-local potential are similar to the binding energies obtained from Ref. [12] within 10%. Figure 1 shows the proton charge densities obtained from our work for  $^{16}\text{O}$ ,  $^{40}\text{Ca}$ , and  $^{208}\text{Pb}$ . The solid (black) and dashed (blue) lines are the proton charge densities for the local and the non-local potentials, respectively. The experimental charge densities for  $^{16}\text{O}$ ,  $^{40}\text{Ca}$ , and  $^{208}\text{Pb}$  are shown by the filled (red) circles [16, 17]. A detailed description of the parameters of  $^{208}\text{Pb}$  used in this work is located in Ref. [13].

Negele (Figs. 4 and 5 of Ref. [18]) calculated the charge density distributions for  $^{16}\text{O}$ ,  $^{40}\text{Ca}$ , and  $^{208}\text{Pb}$  from several theoretical methods, these are; the ordinary Hartree-Fock (HF) theory without the density dependence, the density-dependent HF theory with the bare effective interaction, and the density-dependent HF theory with the interaction obtained from the adjustable parameters, respectively. From these figures, we find that our theoretical results are similar to the calculations of the ordinary Hartree-Fock (HF) without the density dependence by Negele. In Fig. 1, one interesting point is that the proton charge densities of the non-local potential are repulsive at  $r \geq 2$  fm,  $r \geq 3$  fm, and  $r \geq 6$  fm for  $^{16}\text{O}$ ,  $^{40}\text{Ca}$ , and  $^{208}\text{Pb}$ , respectively, due to the non-local effect. At  $r < 2$  fm,  $r < 3$  fm, and  $r < 6$  fm, in contrast, the proton charge densities of the non-local potential are attractive. This result is similar to Ref. [7]. Another interesting point is that the charge density is more repulsive at outer regions with heavier nuclei, as shown in Fig. 1. Figure 2 shows the potentials generated by the local potential and the TELP for the outermost proton and neutron orbits of  $^{16}\text{O}$ ,  $^{40}\text{Ca}$ , and  $^{208}\text{Pb}$  nuclei, respectively. Although the outermost neutron orbit for  $^{208}\text{Pb}$  nuclei is  $3p_{1/2}$ , we choose the  $3s_{1/2}$  orbit to be the same as the outermost proton orbit. Note that the non-local potential is also repulsive at  $r \geq 2$  fm,  $r \geq 3$  fm, and  $r \geq 6$  fm for  $^{16}\text{O}$ ,  $^{40}\text{Ca}$ , and  $^{208}\text{Pb}$ , respectively. Because the non-local potential cannot be directly drawn, we utilized the TELP method, which is used as a non-local potential. Compared with the local potential, the TELP potential is also repulsive.

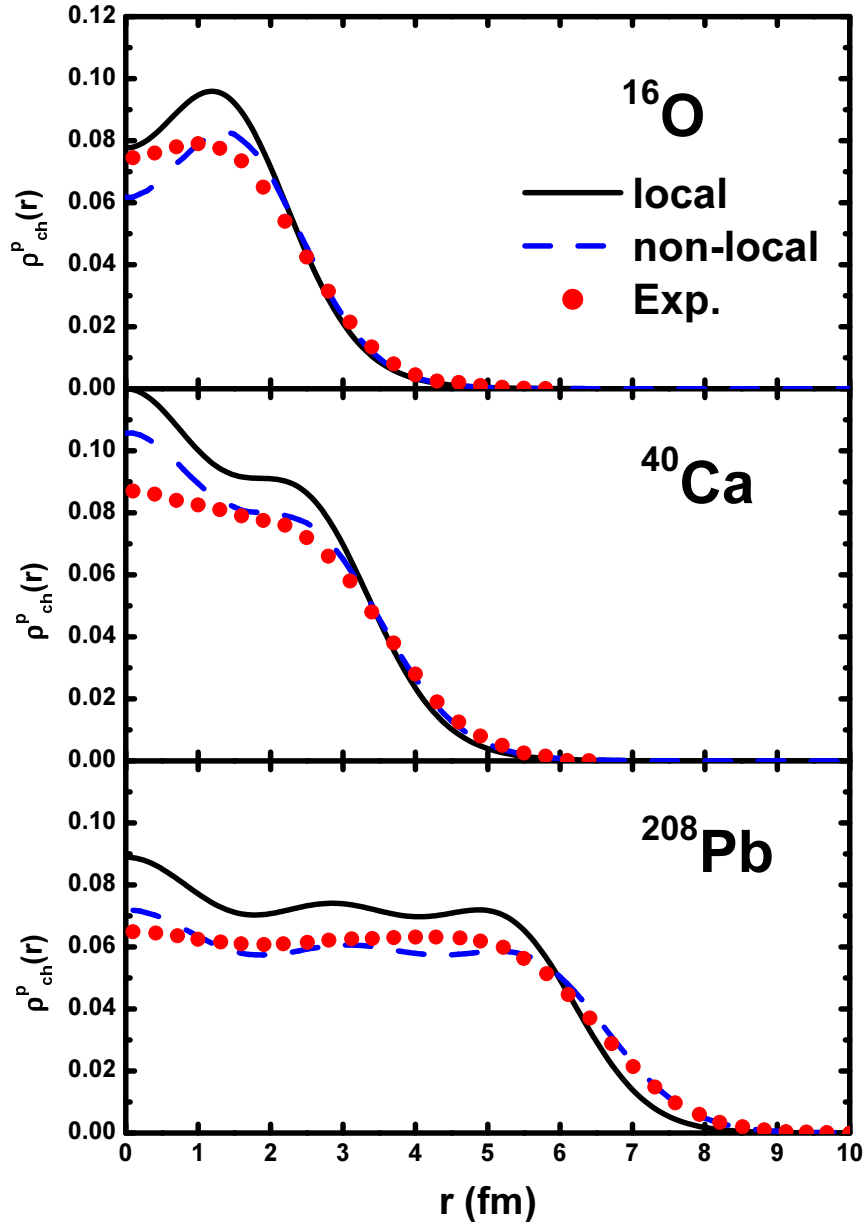


FIG. 1: (Color online) The proton charge density for  $^{16}\text{O}$ ,  $^{40}\text{Ca}$ , and  $^{208}\text{Pb}$ . The solid (black) and the dashed (blue) lines denote the proton charge density obtained from the local and the non-local potential, respectively. The experimental charge densities for  $^{16}\text{O}$ ,  $^{40}\text{Ca}$ , and  $^{208}\text{Pb}$  are also shown by the filled (red) circles [16, 17].

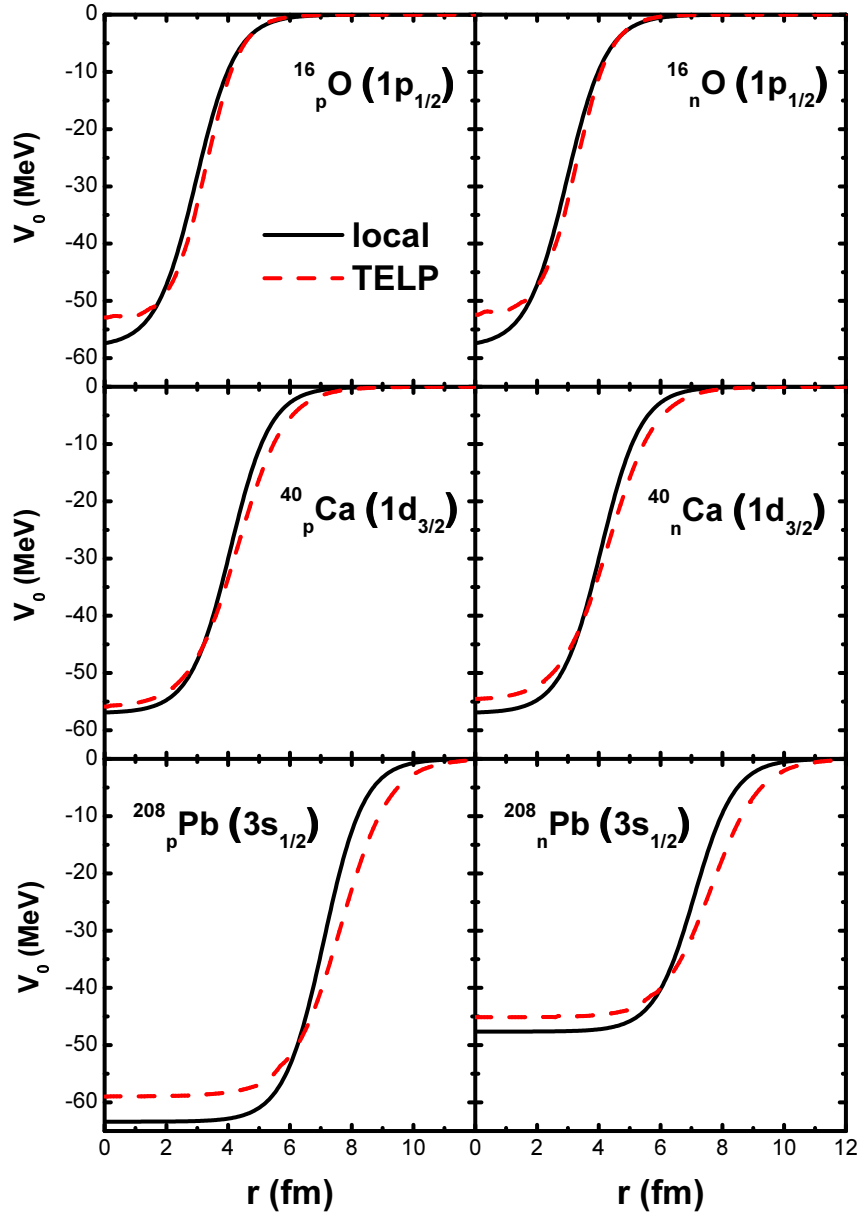


FIG. 2: (Color online) The local (black) potential and the trivially equivalent local potential (red) of the outermost proton and neutron orbits for the  $^{16}\text{O}$ ,  $^{40}\text{Ca}$ , and  $^{208}\text{Pb}$  nuclei, respectively.

Using the integral equation derived from the Schrödinger equation, we calculate the binding energies and wave functions of the nuclear single particle for the non-local potential on the light nuclei such as  $^{16}\text{O}$  and  $^{40}\text{Ca}$  and also obtained charge densities for  $^{16}\text{O}$ ,  $^{40}\text{Ca}$ , and  $^{208}\text{Pb}$ .



In conclusion, the proton charge densities of the non-local potential are repulsive due to the non-local effect, and the non-local potentials are also repulsive in comparison to the local potential.

## References

- [1] H. Feshbach, *Ann. Phys. (N. Y.)* **5**, 357 (1958). doi: 10.1016/0003-4916(58)90007-1
- [2] A. L. Fetter and J. D. Walecka, *Quantum theory of Many-Particle Systems* (McGraw-Hill, New York, 1971), Chap. 4.
- [3] R. S. Mackintosh and S. G. Cooper, *Nucl. Phys. A* **494**, 123 (1989). doi: 10.1016/0375-9474(89)90201-7
- [4] I. J. Thompson, M. A. Nagarajan, J. S. Lilley, and M. J. Smithson, *Nucl. Phys. A* **505**, 84 (1989).
- [5] B. T. Kim and T. Udagawa, *Phys. Lett. B* **273**, 37 (1991). doi: 10.1016/0370-2693(91)90549-6
- [6] W. G. Love, *Nucl. Phys. A* **312**, 160 (1978). doi: 10.1016/0375-9474(78)90582-1
- [7] W.-Y. So and B.-T. Kim, *J. Kor. Phys. Soc.* **30**, 175 (1997).
- [8] F. Perey and B. Buck, *Nucl. Phys.* **32**, 353 (1962). doi: 10.1016/0029-5582(62)90345-0
- [9] M. A. Franey and P. J. Ellis, *Phys. Rev. C* **23**, 787 (1981). doi: 10.1103/PhysRevC.23.787
- [10] J. W. Negele, *Phys. Rev. C* **9**, 1054 (1974). doi: 10.1103/PhysRevC.9.1054
- [11] G. R. Satchler, *Direct Nuclear Reactions* (Clarendon, Oxford, 1983), p. 654.
- [12] S. Shlomo and G. Bertsch, *Nucl. Phys. A* **243**, 507 (1975).
- [13] W. Y. So *et al.*, *J. Kor. Phys. Soc.* **62**, 1703 (2013).
- [14] D. Vautherin and D. Brink, *Phys. Rev. C* **5**, 626 (1972). doi: 10.1103/PhysRevC.5.626
- [15] B. A. Brown, S. E. Massent, and P. E. Hodgson, *J. Phys. G* **5**, 1655 (1979). doi: 10.1088/0305-4616/5/12/008
- [16] W. A. Richter and B. A. Brown, *Phys. Rev. C* **67**, 034317 (2003). doi: 10.1103/PhysRevC.67.034317
- [17] H. J. Emrich, Ph.D. thesis, (University of Mainz, 1983).
- [18] J. W. Negele, *Phys. Rev. C* **1**, 1260 (1970). doi: 10.1103/PhysRevC.1.1260